1964ApJ...140..510S

EVOLUTION OF O STARS. II. HYDROGEN EXHAUSTION AND GRAVITATIONAL CONTRACTION

RICHARD STOTHERS*
Goddard Institute for Space Studies
National Aeronautics and Space Administration
Received February 28, 1964; revised April 22, 1964

ABSTRACT

The evolution of a star of 30 $M_\odot$ is considered from the end of the stable phase of hydrogen burning to the onset of helium burning. Ten models are constructed for the hydrogen-exhaustion (E) phase, and six models for the gravitational contraction (G) phase.

The time scale of the E-phase is so short (8.8×10^4 years) that the shell source remains peaked at $q = 0.34$ and undergoes little hydrogen depletion. Because radiation pressure remains strong in the core, convection does not vanish when the hydrogen content at the center falls to zero. Gravitational contraction of the core contributes more to the luminosity than shell burning, but since the total luminosity changes little, the structure of the envelope is hardly affected. On the H-R diagram, the evolutionary track turns back toward the main sequence when $X_c = 0.03$, and does not turn away again until the shell source becomes important.

The G-phase begins when $L_{\mathrm{H,\,core}}/L < 0.001$, and lasts 9×10^3 years. Although the temperature in the shell increases, hydrogen depletion remains negligible because of the short time scale. However, the shell narrows considerably and its peak moves slightly inward for a while. The steep temperature gradient outside the shell causes the semiconvective zone to move inward to $q = 0.48$; the hydrogen discontinuity attains a value $\Delta X = 0.1$. As the luminosity and radiation pressure in the shell simultaneously increase, the envelope expands. The shell then behaves like a node, since the core continues to contract. The convective region near the center shrinks asymptotically to a value $q = 0\ 06$, but at no time does the core approach an isothermal condition. The gravitational energy release is nearly uniform throughout the core in all phases. At the onset of helium burning, $T_c = 1.5 \times 10^8$ ° K and $\rho_c = 270$ gm/cm^3. Because of the brightening shell source, the stellar radius increases rapidly, bringing the evolutionary track to completion of the typical S-shaped curve on the H-R diagram.

When helium starts to burn, the spectral type is B3, and the star is expected never to return to the region of O stars during its active life.

I. INTRODUCTION

In massive stars when the central hydrogen content falls to a value of 0.03, the whole structure undergoes a drastic reorganization. Kushwaha (1957) first considered the subsequent early phase of hydrogen burning in a shell outside the convective core for a star of 10 $M_\odot$. Reiz (1963) has reconsidered and extended this work, but Hayashi and Cameron (1962) and Hayashi, Hoshi, and Sugimoto (1962) have pursued the study of a star of 15.6 $M_\odot$ into the entire hydrogen-exhaustion phase and then into the gravitational contraction phase preceding helium burning. These phases have also been considered for stars of intermediate mass, as follows: 3.89 $M_\odot$ (Hoyle 1960), 4 $M_\odot$ (Hayashi, Nishida, and Sugimoto 1962; Hayashi, Hoshi, and Sugimoto 1962), 5 $M_\odot$ (Polak 1962), and 7 $M_\odot$ (Hofmeister, Kippenhahn, and Weigert 1963). It is the purpose of the present paper to follow the evolution of a star of 30 $M_\odot$ during these phases to the onset of helium burning at the center. The previous hydrogen-burning stage has been computed in Paper I (Stothers 1963).

II. ASSUMPTIONS AND DEFINITIONS

a) Assumptions

The same general assumptions as in Paper I are made, except that nuclear-energy generation also occurs in a radiative shell around the core and the time rate of change of the physical variables must be taken into account during these fast evolutionary phases.

* This paper and Paper I were based on the author's doctoral dissertation, Harvard University, 1963.

© American Astronomical Society • Provided by the NASA Astrophysics Data System

1964ApJ...140..510S

The opacity of stellar material is again assumed to be due only to electron scattering, and the equation of state is represented by the sum of the perfect gas pressure and radiation pressure.

b) Notation

In general, we apply the same notations for stellar zones as in Paper I, except here we divide the radiative intermediate zone into outer (Zone IIIa) and inner (Zone IIIb) subzones, separated by the radiative, hydrogen-burning shell (denoted by a subscript s).

To designate the successive evolutionary phases we introduce H (hydrogen burning), E (hydrogen exhaustion), and G (gravitational contraction) followed by a number indicating the particular model in the phase.

c) Chemical Composition

The outer radiative envelope retains the initial age-zero composition assumed in Paper I:

$$X_e = 0.70, \qquad Y_e = 0.27, \qquad Z_e = 0.03, \qquad X_{\mathrm{CNO}} = Z_e/2\,. \tag{1}$$

The semiconvective zone constantly adjusts its composition to maintain convective neutrality. A discontinuity in X marks its interface with the inner radiative zone, which retains a constant gradient in X, left behind by the retreating, homogeneous convective core. The distribution of X for the last model of the hydrogen-burning phase is given by Figures 3 and 4 of Paper I. In the core of that model $X_c = 0.07$.

The change of hydrogen content as an explicit function of time, τ, and mass fraction, q, is given by

$$\frac{\partial X}{\partial \tau} = -\frac{\epsilon_{\mathrm{H}}}{E_{\mathrm{H}}} \text{ (radiative region)} \tag{2}$$

and

$$\frac{\partial X}{\partial \tau} = -\frac{1}{q_4 E_{\mathrm{H}}} \int_0^{q_4} \epsilon_{\mathrm{H}} dq \text{ (convective core)}\,, \tag{3}$$

where ϵ_{H} is the energy generation due to hydrogen burning and $E_{\mathrm{H}} = 6.0 \times 10^{18}$ erg/gm is the energy released per CNO cycle.

d) Nuclear Energy

The accurate expression for the rate of energy release due to the conversion of hydrogen into helium via the full CNO cycle has been given by Reeves (1962) in terms of the $N^{14} + H^1$ rate:

$$\epsilon_{\mathrm{H}} = 7.94 \times 10^{27} f_{14\ 1} g_{14\ 1} \left(\frac{X_{14}}{X_{\mathrm{CNO}}}\right) X_{\mathrm{CNO}} X \rho T_6^{-2/3} \exp(-152.3\, T_6^{-1/3}) \quad \text{erg/gm sec} \tag{4}$$

where

$$f_{14,1} = 1 + 1.75\ \rho^{1/2} T_6^{-2/3}\,, \tag{5}$$

$$g_{14,1} = 1 + 0.0027\ T_6^{1/3} - 0.0037\ T_6^{1/6} - 0.00007\ T_6\,, \tag{6}$$

$$X_{14}/X_{\mathrm{CNO}} = 0.99 - 0.00067\ T_6\,. \tag{7}$$

Here $f_{14,1}$ is the weak electron-screening factor, $g_{14,1}$ is the correction term to the zero-energy S factor, and X_{14}/X_{CNO} has been estimated from tables given by Reeves (1962) for temperatures in excess of 2.5×10^7 ° K. We are assuming everywhere the full equilibrium abundance of oxygen, which, strictly speaking, is not attained in the cooler shell source because of the short time scale involved.

© American Astronomical Society • Provided by the NASA Astrophysics Data System

1964ApJ...140..510S

e) Gravitational Energy

The amount of energy involved during a gravitational contraction or expansion is expressed as the difference between the work done by the pressure and the change in thermal energy of the gas and radiation:

$$\epsilon_g = -P\frac{\partial v}{\partial \tau} - \frac{\partial u}{\partial \tau} = \tfrac{3}{2}\frac{kT}{\mu H}\left[\frac{\partial}{\partial \tau}\ln(Ty^{-2/3}e^{-8y/3}) + \frac{5+8y}{3}\frac{\partial}{\partial \tau}\ln \mu\right], \tag{8}$$

where

$$v = \frac{1}{\rho}, \qquad \frac{u}{v} = \tfrac{3}{2}\frac{k}{\mu H}\rho T + aT^4, \qquad y = \frac{1-\beta}{\beta}, \tag{9}$$

and the time derivative applies to a given mass fraction. As Hayashi and Cameron (1962) have noted, the logarithmic arguments in equation (8) are independent of position in convective regions of the star.

III. BASIC EQUATIONS

The basic equilibrium equations are given in Paper I. For Zones I–IIIa the equations were transformed and integrated, and the zones fitted to each other in the same way as before. Henceforth we shall call this region simply the *envelope*. It is specified only by the luminosity L (through the parameter C) since, down to the chosen termination point $q_f = 0.500$, the composition in the radiative region has been fixed by the previous models.

In the *core* (Zones IIIb and IV) we employ q as the independent variable and logarithms of r, $L(r)$, P, and T as dependent variables. The core solutions are specified by β_c and T_c and are integrated from the center out through the shell to q_f, beyond which any energy sources are negligible. The customary series expansions near the center (Schwarzschild [1958], p. 114) have been modified to include radiation pressure and applied at $q = 0.002$. The step value was taken to be $\Delta q = 0.001$.

Fitting of the envelope and core is made at q_f in U, V, and $L(r) = L$. Since L was expected to change little during the present evolutionary phases, it was sufficient to integrate a short series of envelopes at equally spaced intervals of L and then to interpolate values of U_f and V_f at finer intervals of L.

The change in $X(q)$ as a function of time has been given by equations (2) and (3). These may be approximated by difference equations, with the known run of (ϵ_H/X) as a function of q from the previous model. Letting ι refer to quantities of the previous model, we write in an obvious notation

$$\frac{\Delta \ln X}{\Delta \tau} = -\frac{1}{2E_{\mathrm{H}}}\left[\left(\frac{\epsilon_{\mathrm{H}}}{X}\right)^{\iota} + \left(\frac{\epsilon_{\mathrm{H}}}{X}\right)\right] = -\Xi_r(q), \qquad (q \geq q_4{}^{\iota}) \tag{10}$$

$$\frac{\Delta \ln X}{\Delta \tau} = -\frac{1}{(q_4{}^{\iota} + q_4)E_{\mathrm{H}}}\int_0^{q_4}\left[\left(\frac{\epsilon_{\mathrm{H}}}{X}\right)^{\iota} + \left(\frac{\epsilon_{\mathrm{H}}}{X}\right)\right]dq = -\Xi_c(q_4), \quad (q_4 \geq q > 0) \tag{11}$$

$$\frac{\Delta \ln X}{\Delta \tau} = \Xi_r(q) + [\Xi_c(q_4) - \Xi_r(q_4)]\frac{q_4{}^{\iota} - q}{q_4{}^{\iota} - q_4}, \qquad (q_4{}^{\iota} \geq q \geq q_4) \tag{12}$$

for $q_4{}^{\iota} - q_4$ small. These approximations are slightly more accurate than those used by Haselgrove and Hoyle (1956) and by Hayashi and Cameron (1962). Outside the convective core, in which X_c is known (constant), an iterative procedure must be used to calculate X from equation (10) or equation (12), since $(\epsilon_{\mathrm{H}}/X)$ depends implicitly on X through ρ. Using X from the previous model, we calculate a preliminary value of ρ and hence $(\epsilon_{\mathrm{H}}/X)$. Insertion of $(\epsilon_{\mathrm{H}}/X)$ into equations (10) or (12) yields a projected value

© American Astronomical Society • Provided by the NASA Astrophysics Data System

1964ApJ...140..510S

of X. Repetition of this procedure yields a definitive value of X correct to the second order.

The method of producing an evolutionary step was varied according to the magnitude of the ratio of luminosity supplied by gravitational contraction to total luminosity, as follows.

a) $L_g/L < 0.1$

The method of Hayashi and Cameron (1962) was adopted for this case only, although they seem to have used it up to $L_g/L \approx 0.6$. Here the part of the gravitational energy release inclosed in brackets in equation (8) is expressed as a quadratic function of q, with coefficients extrapolated from the previous models:

$$\epsilon_g = \frac{3}{2}\frac{kT}{\mu H}(a_0 + a_1 q + a_2 q^2) \; . \tag{13}$$

The basic equations, where now $\epsilon = \epsilon_{\mathrm{H}} + \epsilon_g$, are integrated from the center with input values of X_c, β_c, T_c, a_0, a_1, a_2, $q_4{}'$, and the run of X' and $(\epsilon_{\mathrm{H}}/X)'$ as a function of q. At q_4, $\Delta\tau$ is determined by equation (11). When a self-consistent model is obtained, the quantity in brackets in equation (8) is computed exactly and improved values of a_0, a_1, and a_2 are obtained by least squares. Another model is integrated with the new values, but this second model is always sufficiently accurate for $L_g/L < 0.1$.

b) $0.1 < L_g/L < 0.5$

In this case we specify X_c and estimate $\Delta\tau$ by extrapolation from the previous models. Hence ϵ_g can be computed exactly from equation (8) with the given $\Delta\tau$. In the course of integrations to find the correct β_c and T_c it is possible continually to improve $\Delta\tau$ by use of equation (11).

c) $L_g/L > 0.5$

As L_g/L increases, L becomes more sensitive to ϵ_g and hence to $\Delta\tau$. To cope with the increasing difficulty of making $\Delta\tau$ converge, we choose a parameter that loses importance with increasing L_g/L, namely, X_c. In this case, we take the time step by specifying $\Delta\tau$ explicitly. With a value of X_c extrapolated from the previous models, it is possible to obtain a definitive value for X_c in the same way as for $\Delta\tau$ in Section III*b*. Eventually, when hydrogen burning ceases entirely in the shrinking convective core, we need only specify $\Delta\tau$.

IV. HYDROGEN-EXHAUSTION PHASE

The results of the computations for this phase are presented in Table 1. It is curious that the stellar radius starts to decrease, causing the star to turn back toward the main sequence in the H-R diagram, as soon as $X_c \approx 0.03$ for a broad range of stellar masses ($10 < M/M_\odot < 60$), even though the mass fractions contained in the convective core are very different (see Table 2). It is clear, however, why the radius will shrink when X_c becomes small. To maintain the luminosity, the central temperature must correspondingly increase; but since μ_c changes little, $R \sim T_c^{-1}$ from equation (10) of Paper I.

For a while hydrogen burning in the core is able, alone, to maintain the energy balance (Schwarzschild and Härm 1958). However, eventually an accelerated contraction of the core is necessary to supplement the deficient $L_{\mathrm{H,\,core}}$ with a growing L_g. When the temperature becomes high enough, hydrogen burning in a shell outside the core also becomes important. It is interesting to note that in the above range of masses the peak of this shell source always coincides with the mass fraction of the convective core when $X_c \approx 0.07$, i.e., just *before* the radius starts to decrease. Table 2 shows that q_s, the peak of the shell source, is roughly half of q_0, the mass fraction of the core of the initial main-sequence model. Furthermore, q_0 itself increases by about 0.15 every time the stellar

© American Astronomical Society • Provided by the NASA Astrophysics Data System

1964ApJ...140..510S

mass is doubled; this is a consequence of the increasing importance of radiation pressure (diminishing β), which extends the convective regions outward.

It is for this reason, the very distance of the hydrogen-rich regions, that the temperature at $X \approx 0.07$ is low and shell burning is consequently delayed. (In massive stars, β is low not so much by virtue of high temperature as of low density.) In stars of lower mass the point at which $X_c \approx 0.07$ lies closer to the center, and shell burning begins to contribute significantly to the luminosity before the core contraction does. The critical mass for this to happen is about 20 $M_\odot$. If q_s is small enough that the core mass lies below the Schönberg-Chandrasekhar limit ($q \approx 0.1$), thus becoming isothermal or even degenerate, then L_g may always be small. The approach to isothermality may be seen in a plot of log T against q for 5 $M_\odot$ (Polak 1962, Fig. 3), where $q_s = 0.11$. It may be inferred for 15.6 $M_\odot$ (Hayashi and Cameron 1962), where $q_s = 0.17$, since $L_{\mathrm{H,\,shell}} > L_g$ until $X_c < 0.001$. In stars with mass ~ 1 $M_\odot$ (Schwarzschild and Selberg 1962), the

TABLE 1

EVOLUTIONARY MODELS OF A STAR OF 30 $M_\odot$ DURING HYDROGEN-EXHAUSTION (E) PHASE

	Models									
	1	2	3	4	5	6	7	8	9	10
log C	−3 272	−3 266	−3 264	−3 262	−3 260	−3 256	−3 252	−3 248	−3 244	−3 239
q_1	+0 717	+0 719	+0 720	+0 721	+0 721	+0 722	+0 723	+0 725	+0 728	+0 731
$q_2 = q_3$	+0 550	+0 547	+0 546	+0 545	+0 545	+0 543	+0 541	+0 539	+0 537	+0 534
X_2	+0 650	+0 647	+0 645	+0 644	+0 643	+0 640	+0 637	+0 634	+0 630	+0 627
X_3	+0 589	+0 584	+0 581	+0 579	+0 578	+0 573	+0 568	+0 564	+0 559	+0 554
q_s	+0 342	+0 342	+0 342	+0 342	+0 342	+0 342	+0 342	+0 342	+0 342	+0 342
β_s	+0 614	+0 608	+0 605	+0 605	+0 604	+0 604	+0 602	+0 600	+0 597	+0 595
log T_s	+7 436	+7 458	+7 487	+7 515	+7 542	+7 561	+7 571	+7 578	+7 584	+7 589
log $(r_s/R_\odot)$	+0 267	+0.240	+0 211	+0 181	+0 153	+0 130	+0 117	+0 107	+0 097	+0 089
q_4	+0 328	+0 320	+0 316	+0 311	+0 302	+0 282	+0 258	+0 236	+0 205	+0 182
log X_c	−1 523	−2 023	−2 523	−3 023	−3 523	−4 023	−4 523	−5 015	−5 882	−7 311
β_c	+0 564	+0 557	+0 554	+0 555	+0 555	+0 559	+0 563	+0 567	+0 572	+0 577
log T_c	+7 665	+7 696	+7 726	+7 756	+7 785	+7 808	+7 823	+7 833	+7 844	+7 854
log ρ_c	+0 701	+0 795	+0 886	+0 978	+1 066	+1 140	+1 193	+1 229	+1 272	+1 312
$L_{H,\,\mathrm{core}}/L$	+0 999	+0 995	+0 985	+0 943	+0 853	+0 599	+0 319	+0.145	+0 028	+0 002
$L_{H,\,\mathrm{shell}}/L$	. . . .	+0 001	+0 004	+0 014	+0 044	+0 094	+0 141	+0 175	+0 217	+0 249
L_g/L	+0 001	+0 004	+0 011	+0 043	+0 103	+0 307	+0 540	+0 680	+0 755	+0 749
log $(L/L_\odot)$	+5 439	+5 445	+5 447	+5 449	+5 451	+5 455	+5 459	+5 463	+5 468	+5 472
log $(R/R_\odot)$	+1 143	+1 136	+1 113	+1 090	+1 066	+1 057	+1 057	+1 062	+1 070	+1 079
log T_e	+4 548	+4 554	+4 565	+4 578	+4 590	+4 595	+4 596	+4 595	+4 592	+4 589
τ (10^4 years)	0 00	+5 91	+7 74	+8 33	+8 53	+8 60	+8 64	+8 67	+8 69	+8 72

TABLE 2

LOCATION OF CRITICAL INTERFACES IN STARS OF INTERMEDIATE AND HIGH MASS WHEN $X_c \approx$ 0 03

$M/M_\odot$	q_0	q_s	q_4	X_e	Reference
5	0 21	0 11	0 10	0 74	Polak (1962)
10	24	.	07	90	Kushwaha (1957)
15 6	42	17	16	90	Sakashita, Ôno, Hayashi (1959)
30 .	60	0 34	33	70	Stothers (1963)
62 7	0 75		0 44	0 75	Schwarzschild and Härm (1958)

© American Astronomical Society • Provided by the NASA Astrophysics Data System

1964ApJ...140..510S

shell source supplies practically all the luminosity outside a very large degenerate core. The critical stellar mass for the occurrence of degeneracy in the core prior to helium burning is $\sim 4\ M_\odot$ (Hayashi, Nishida, and Sugimoto 1962).

At $30\ M_\odot$, $q_s \gg 0.1$ and the core never even approaches an isothermal condition. Thus gravitational contraction proceeds unchecked to increase T_c in accordance with the virial theorem. The subsequent increase in ϵ_H reduces X_c to less than 1 per cent. Thereafter the drop in X_c outruns the increase in T_c^ν, and ϵ_H decreases, being supplanted by $\epsilon_g \sim \partial T_c/\partial \tau$. However, hydrogen burning in the core still supplies over half the total luminosity even when X_c is as low as 10^{-4}.

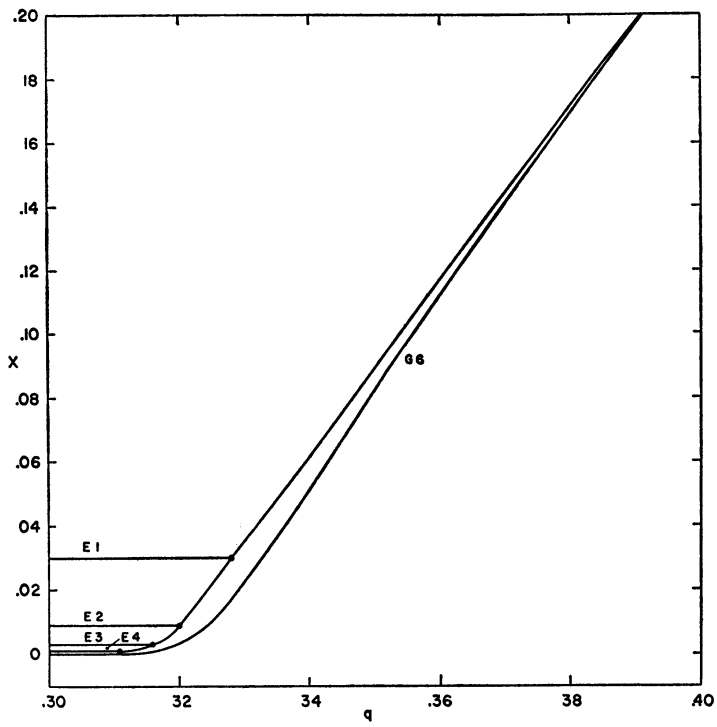

FIG. 1.—Depletion of hydrogen as a function of mass fraction during the hydrogen-exhaustion (E) and gravitational-contraction (G) phases. Filled circles represent the boundary of the convective core in the E models.

The distribution of hydrogen in the central regions may be seen in Figure 1. It is clear that, because of the high central temperature and the luminosity requirements, X_c begins to decrease more and more rapidly with q_4. This has the effect of necessitating an even sharper increase of temperature, which consequently exhausts the central hydrogen and ignites a region which is still relatively hydrogen-rich but close enough to the center to feel the temperature rise. Thus Figure 1 shows why a shell source develops near $q = 0.34$ for $30\ M_\odot$. We expect this shell to be initially broader in massive stars than in stars of lower mass because the mean gradient of hydrogen throughout this region is gentler (larger $q_0 - q_s$; see Table 2). The subsequent growth of the shell source is shown in Figure 2.

In Figure 3 the relative contributions to the energy generation may be compared. The magnitude of ϵ_g is very nearly constant throughout the core for all stages.

Shrinkage of the convective core is at first slow because β_c remains almost constant. Hence the evolution of the center approximates Lane's law, $\rho_c \sim T_c^3$. When the shell

© American Astronomical Society • Provided by the NASA Astrophysics Data System

1964ApJ...140..510S

source becomes important for $X_c < 10^{-4}$, ρ_c increases at a slightly greater rate than T_c^3, the only concession to isothermality that the core makes. At this point (Model E7), $L_g/L \approx 0.5$ and $L_{\mathrm{H,\,shell}}/L \approx 0.1$. It seems that as soon as L_g/L grows much larger, contraction of the core begins to be offset by an expansion of the envelope (cf. Hayashi and Cameron 1962). This expansion is due to an increase of $L_{\mathrm{H,\,shell}}$, compensating for the reduction of $L_{\mathrm{H,\,core}}$. Exactly why the envelope expands as $L_{\mathrm{H,\,shell}}$ increases will be made evident in the next section. The result on the H-R diagram is that the star takes another turn away from the main sequence.

When the hydrogen content at the center of the star vanishes after Model E10, the convective core does not disappear. This contrasts with the results on stars of lower mass (Hoyle 1960; Polak 1962; Hayashi and Cameron 1962), where apparently it is

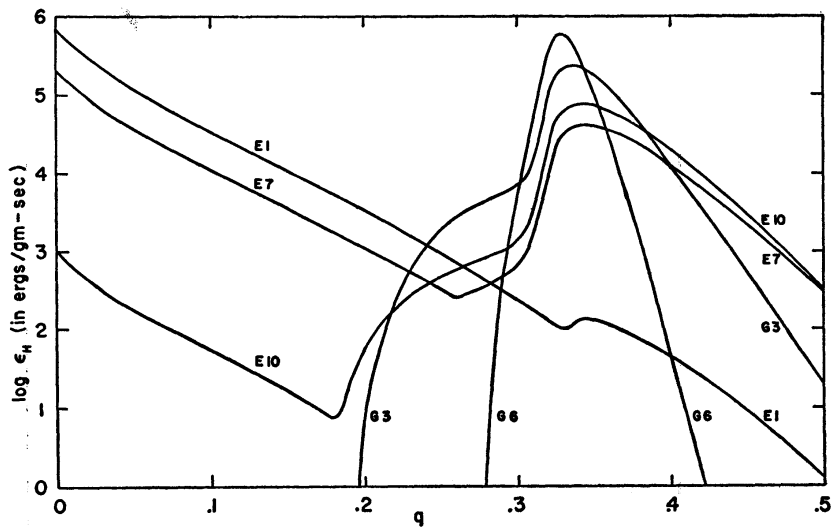

FIG. 2.—Logarithm of the energy generation due to hydrogen burning as a function of mass fraction. Curves are labeled with the model numbers.

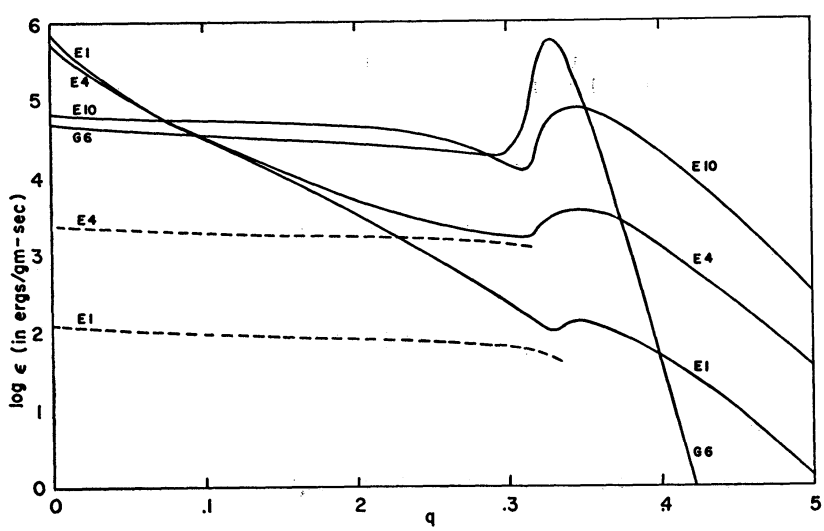

FIG. 3.—Logarithm of the energy generation as a function of mass fraction. Solid curves refer to the contributions from both hydrogen burning and gravitational contraction. The dashed curve refers only to gravitational contraction. Curves are labeled with the model numbers.

© American Astronomical Society • Provided by the NASA Astrophysics Data System

1964ApJ...140..510S

just the nuclear-energy generation that maintains the steep temperature gradient. However, in the case of 30 $M_\odot$, β is still so low that convection persists near the center.

The time scale of this phase is short enough (8.8×10^4 years) that the shell source, which remains peaked at $q_s = 0.342$, undergoes very little hydrogen depletion. Because of the struggle of the various energy sources to maintain the luminosity, L increases but slightly. Thus the structure of the envelope remains nearly constant.

V. GRAVITATIONAL CONTRACTION PHASE

This phase is taken to start when $L_{H,\,\mathrm{core}}/L < 0.001$. The hydrogen content of the convective core is negligible, and the sole nuclear-energy source is the hydrogen-burning shell. In Model E9 the rise of the shell source had terminated the upward growth of

TABLE 3

EVOLUTIONARY MODELS OF A STAR OF 30 $M_\odot$ DURING GRAVITATIONAL CONTRACTION (G) PHASE

	Models					
	1	2	3	4	5	6
log C	−3 231	−3 216	−3 195	−3 178	−3 165	−3 152
q_1	+0 733	+0 739	+0 749	+0 756	+0 762	+0 769
$q_2 = q_3$	+0 530	+0 522	+0 508	+0 498	+0 489	+0 481
X_2	+0 620	+0 606	+0 582	+0 560	+0 541	+0 522
X_3	+0 542	+0 523	+0 490	+0 467	+0 445	+0 425
q_s	+0 342	+0 342	+0 338	+0 328	+0 328	+0 328
β_s	+0 589	+0 576	+0 556	+0 553	+0 553	+0 515
log T_s	+7 596	+7 607	+7 626	+7 654	+7 668	+7 683
log $(r_s/R_\odot)$	+0 073	+0 048	+0 001	−0 058	−0 100	−0 142
q_4	+0 155	+0 123	+0 093	+0 078	+0 069	+0 064
β_c	+0 587	+0 604	+0 631	+0 651	+0 665	+0 674
log T_c	+7 873	+7 907	+7 971	+8 035	+8 101	+8 168
log ρ_c	+1 386	+1 520	+1 760	+1 992	+2 217	+2 433
$L_{H,\,\mathrm{shell}}/L$	+0 307	+0 391	+0 485	+0 536	+0 561	+0 575
L_g/L	+0 693	+0 609	+0 515	+0 464	+0 439	+0 425
log $(L/L_\odot)$	+5 480	+5 495	+5 516	+5 533	+5 546	+5 560
log $(R/R_\odot)$	+1 098	+1 144	+1 239	+1 353	+1 492	+1 680
log T_e	+4 581	+4 562	+4 520	+4 467	+4 401	+4 310
τ (10^4 years)	0 00	+0 10	+0 30	+0 50	+0 70	+0 90

L_g/L, which reached a maximum value of 0.75. This fraction becomes all the more impressive when we compare it with 0.56 for a star of 15.6 $M_\odot$ (Hayashi and Cameron 1962). Table 3 shows that even at the onset of helium burning (Model G6) the contribution of gravitational contraction to the luminosity is still a sizable fraction. This suggests that for stars more massive than 30 $M_\odot$ hydrogen burning in a shell may not become dominant.

During the shell-burning phases, the computational difficulty of fitting models increases. The reason lies in the shift of the $U - V$ curve to the left, as seen in Figure 4. This is caused by the developing chemical inhomogeneity, which began after the initial main-sequence state, and by the shell source, which produces the leftward loop on the $U - V$ plane. Because of the short time scale, the amount of hydrogen depletion is very small and the shell source remains peaked at roughly the same mass fraction. Since the shell provides the driving mechanism for the expanding envelope while the core is contracting, r at the outer boundary of the shell remains roughly constant. Thus it is here that the change of log r with q is greatest (see Fig. 5), that is, U is a minimum, isolating

© American Astronomical Society • Provided by the NASA Astrophysics Data System

1964ApJ...140..510S

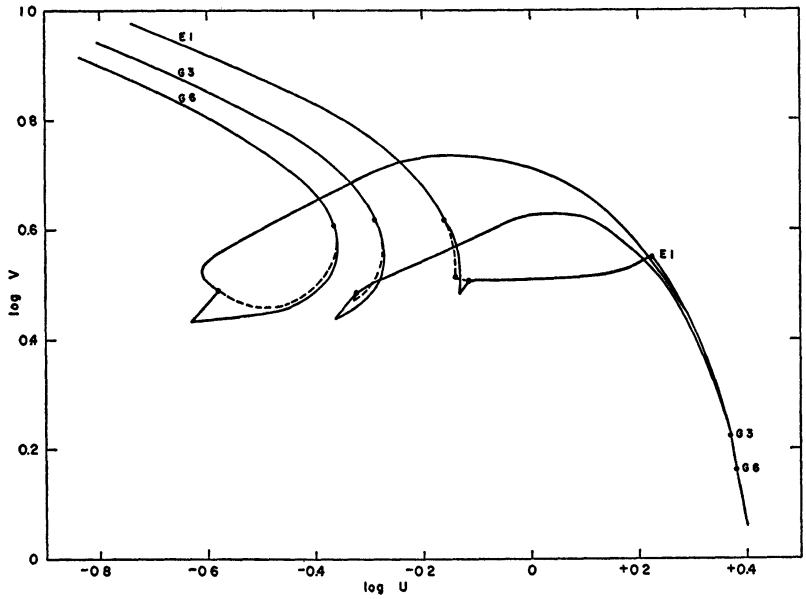

FIG. 4.—Evolution of a star of 30 $M_\odot$ in the $U - V$ plane during the hydrogen-exhaustion (E) and gravitational-contraction (G) phases. Curves are labeled with the model numbers. Dots and jumps represent fitting points. The dashed lines in the solutions represent the assumed radiative zone (see Paper I).

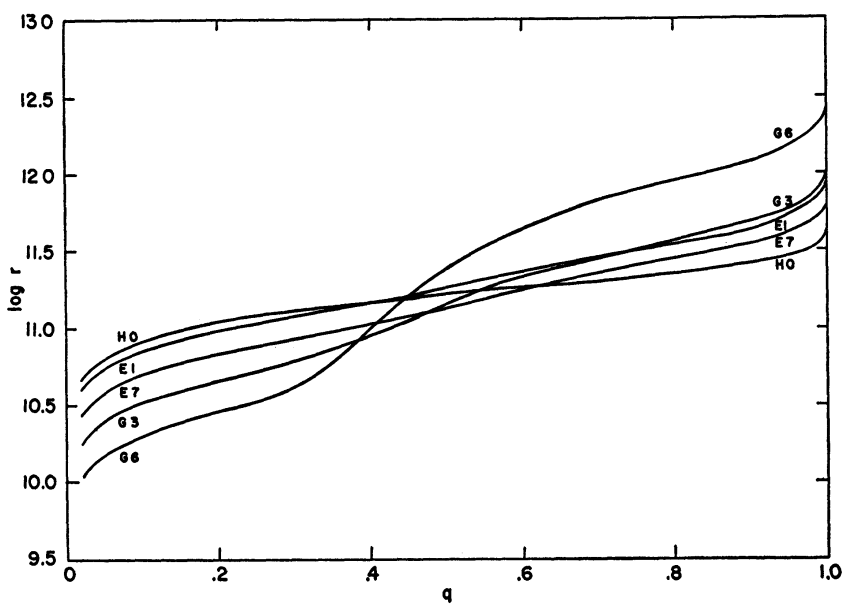

FIG. 5.—Logarithm of the radius as a function of mass fraction. Curves are labeled with the model numbers.

© American Astronomical Society • Provided by the NASA Astrophysics Data System

1964ApJ...140..510S

the energy-producing regions from the envelope. Unless small increments in q are taken in the numerical integrations through the shell, the solutions diverge. Since the region behaves like an outer boundary ($U_s \rightarrow 0$), V tends to blow up for small changes of the input parameters, β_c and T_c.

Hayashi, Hoshi, and Sugimoto (1962) have interpreted the envelope expansion in terms of the $U - V$ plane. For values of the polytropic index $3 \geq N > 1$, where $P = K\rho^{1+1/N}$ and K and N are constants, the centrally condensed solutions of a polytropic envelope form a leftward loop on the $U - V$ plane and converge to a point $U = 0$ and $V = N + 1$ as $r \rightarrow 0$. For an electron-scattering envelope, N is 3 near the surface, decreases inside, and then approaches 3 again as $r \rightarrow 0$. Hence such an envelope approximates the polytropic case $N = 3$, where $V \rightarrow 4$ as $U \rightarrow 0$ (see Fig. 4). Interior to q_s, $L(r) \ll L_{\mathrm{H,\,shell}}$ so that the radiative index becomes large, since $(n + 1)_{\mathrm{rad}} \sim (1 - \beta)/\kappa L(r)$. Hence the core approximates roughly the isothermal case $N = \infty$, which loops outward in the $U - V$ plane much as in Figure 4.

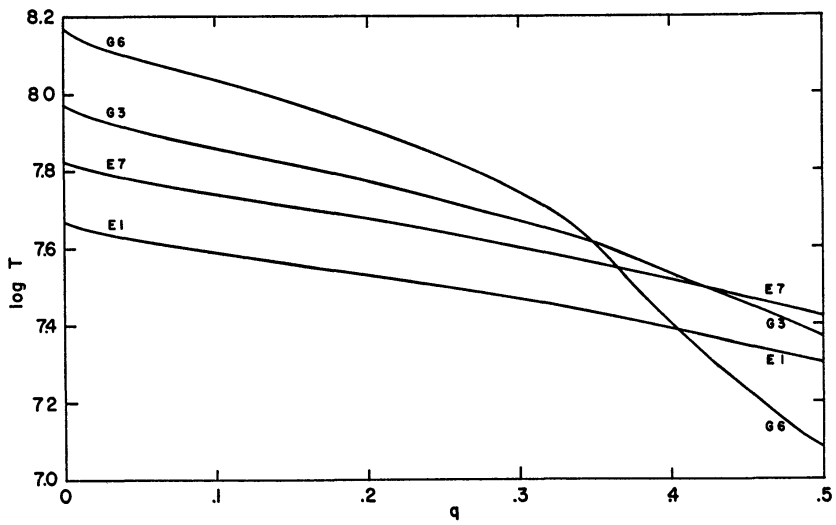

FIG. 6.—Logarithm of the temperature as a function of mass fraction. Curves are labeled with the model numbers.

It remains to see how the shell source actually expands the envelope. We have already noted that, in order to tap additional nuclear fuel, the temperature in the core rises and starts shell burning. Consequent to hydrogen exhaustion in the core, the temperature in the shell must continue to rise so that $L_{\mathrm{H,\,shell}}$ can assume more of the total luminosity burden. As $L_{\mathrm{H,\,shell}}$ increases during the evolution, $(n + 1)_{\mathrm{rad}}$ decreases, steepening the temperature gradient beyond q_s (see Fig. 6). But actually $n + 1$ can only decrease until the adiabatic value is reached. Therefore, to compensate for the increasing luminosity, β decreases (see Fig. 7). This relative increase in radiation pressure expands the envelope.

To make this point more definite, we look at the structure of the envelope, which may be considered a polytrope of some characteristic index. The effective termination point of the envelope must be taken just outside the shell peak, where U is a minimum on the $U - V$ plane. Now it may be shown generally for a polytrope of any index and constant $\beta = \beta_c$ that $R \sim (T_c/\beta_c\rho_c)^{1/2}$. Eliminating ρ, we have $R \sim (1 - \beta_c)^{1/2}/\beta_c T_c$. Thus the expansion may be considered as fundamentally due to the relative increase in radiation pressure, as stated above. Further, the same result can be obtained by examining equation (8). A decrease in β causes expansion by making ϵ_g negative, and an in-

© American Astronomical Society • Provided by the NASA Astrophysics Data System

1964ApJ...140..510S

crease causes contraction by making ϵ_g positive. The consequences may be seen by comparing Figures 5–7. During phases of roughly constant β, the change of T will determine the change in R.

If we take the stellar core to be a polytrope, then we may similarly explain the changes of shell radius, r_s (see Tables 1 and 3). By extension, a star with m shell sources may be subdivided into $m + 1$ zones whose structure is assumed to be polytropic. Then, approximately, the changes of β and T at a given shell should determine the changes of r at the next outer shell, unless the mass fraction of the shell changes by a drastic amount. Qualitative agreement is found between this picture of evolution and the accurate published results on the evolution of stars of 4 $M_\odot$ and 15.6 $M_\odot$ from the initial main sequence through carbon burning (Hayashi, Nishida, and Sugimoto 1962; Hayashi and Cameron 1962; Hayashi, Hoshi, and Sugimoto 1962).

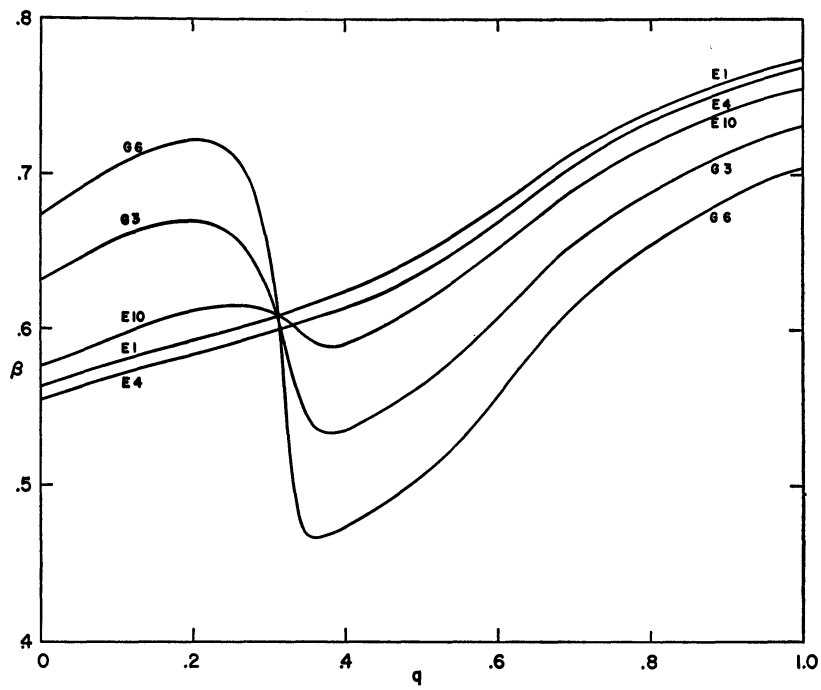

FIG. 7.—Ratio of gas pressure to total pressure as a function of mass fraction. Curves are labeled with the model numbers.

In this regard we note that the last model before helium burning in a star of 1.3 $M_\odot$ considered by Schwarzschild and Selberg (1962) had $\beta_s = 0.87$. Since they neglected radiation pressure and used $\beta = 1$ throughout, it might be expected that the radii they derive are too small. Indeed the track of their theoretical models on the H-R diagram deviates leftward of the observed red-giant branch in globular clusters. One reason may be the neglect of varying β in their models; apart from other factors, for a closer agreement with observations β should be explicitly included.

Since the envelope evolves independently of the core (each with a fixed mass), the expansion of the envelope must lower the local density. Since β is also decreasing in the envelope, the temperature near q_s actually does not change very much (see Fig. 6). Beyond the shell, however, it drops considerably, because the temperature gradient is approaching the adiabatic value. This increase of the temperature gradient has two major effects: (1) The semiconvective zone moves steadily inward; by Model G6 it has reached

© American Astronomical Society • Provided by the NASA Astrophysics Data System

1964ApJ...140..510S

$q = 0.48$. The hydrogen discontinuity grows to $X_2 - X_3 = 0.10$, although $\mu_2/\mu_3 = 0.91$ because the actual hydrogen content is lower at small q. (2) The shell source becomes narrower, on account of the decreasing temperature outside (and the decreasing hydrogen content inside). A curious result, not occurring in stars of lower mass, is that q_s moves slightly inward at first because of the rising temperature inside and the rather broad shell distribution of hydrogen, but thereafter remains stationary as it encounters less and less hydrogen. The total amount of hydrogen depletion (in the shell) is 0.0004, and the maximum local change in X is 0.011 at $q = 0.329$.

In the core, although β_c steadily rises, the central convection persists and recedes only to a roughly constant $q_4 = 0.06$ at the onset of helium burning. Hence convection probably never disappears completely from the center of very massive stars.

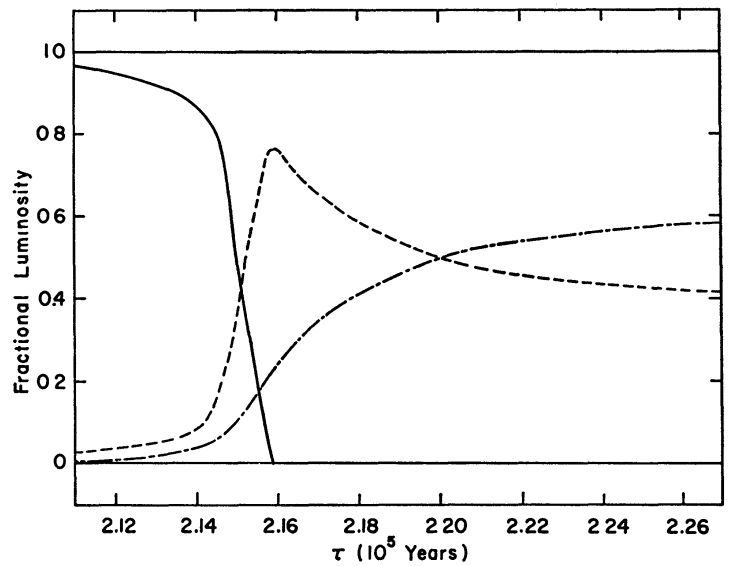

FIG 8 —The fraction of the total luminosity contributed by hydrogen burning in the core (*solid curve*), gravitational contraction in the core (*dashed curve*), and hydrogen burning in the shell (*dash-dot curve*) is plotted against the time elapsed since the last model of the hydrogen-burning phase (Model H4 of Paper I).

Model G6 corresponds to the onset of helium burning. At this point, $L_{He}/L \approx 0.004$ and T_c is 150 million degrees. This value of T_c is almost the same as the corresponding value for a star of 15.6 $M_\odot$ because of the steep temperature dependence of the energy-generation formula. However, ρ_c is only 270 gm/cm^3, lower by a factor of 10 than in the star of 15.6 $M_\odot$. But in the heavier star the core mass is four times as large.

The gravitational contraction phase is very short (9×10^3 years), although large changes in the stellar radius take place.

VI. FINAL REMARKS

Although the computed values of the *fractional* luminosities should not be considered exact (since we have neglected in the computations to take account of the radiative flux that is absorbed in the expansion of the envelope), nevertheless Figure 8 shows up a brief peak in the luminosity due to gravitational contraction, whereas the nuclear-energy sources are spread over longer time intervals. Since the total energy available to the star as a result of gravitational contraction is small compared with the nuclear-energy store, it is expected that the time scale of contraction phases will be very short. Indeed,

© American Astronomical Society • Provided by the NASA Astrophysics Data System

1964ApJ...140..510S

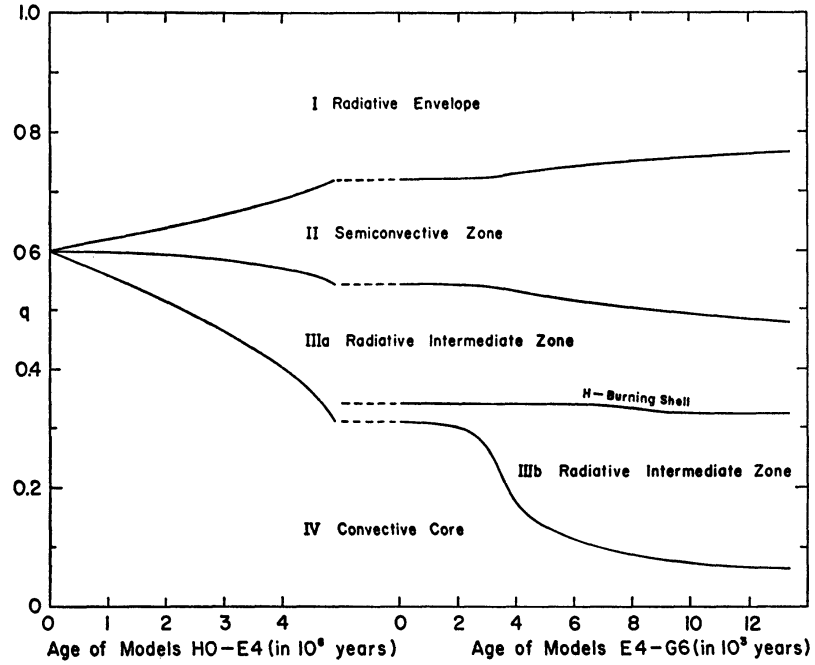

FIG. 9.—Evolution of the structural zones from the initial main sequence to the onset of helium burning.

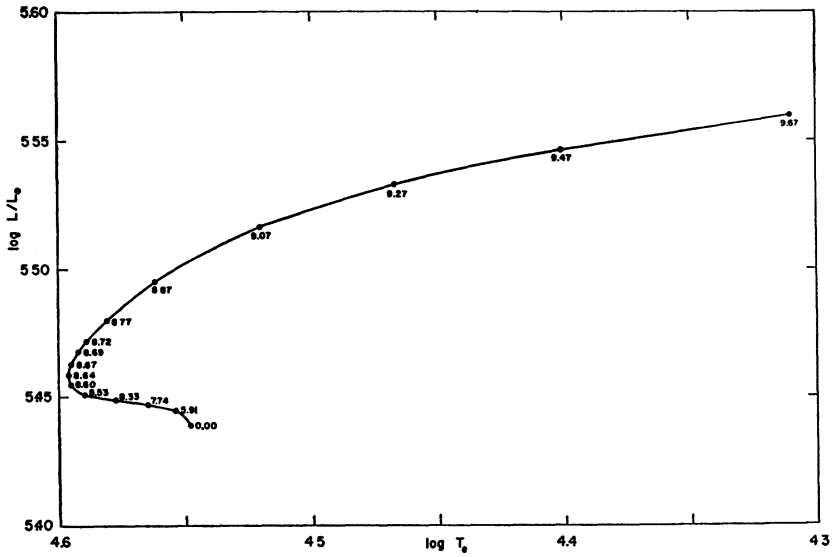

FIG. 10.—Evolution of a star of 30 $M_\odot$ on a plot of luminosity versus effective temperature, during the phases of hydrogen exhaustion and gravitational contraction. Numbers attached to the models (*filled circles*) represent the age in units of 10^4 years.

© American Astronomical Society • Provided by the NASA Astrophysics Data System

1964ApJ...140..510S

the post–main-sequence age at the onset of helium burning is 4.9 million years, of which 4.8 million are spent burning almost half of the initial hydrogen content.

During this time the interior structure of the star undergoes drastic changes, especially in the short (0.1×10^6 years) contraction phase, as shown in Figure 9. One complication not occurring in stars of lower mass may arise from the existence of the semiconvective zone. That is, the inward-moving semiconvection brings hydrogen-enriched material toward the shell source, which is simultaneously moving outward. A hydrogen flare-up might be expected to occur. However, the results of Table 3 show that ΔX is only about 0.1 at the radiative-semiconvective interface. Moreover, from the results on a star of 15.6 $M_\odot$ (Hayashi and Cameron 1962; Hayashi, Hoshi, and Sugimoto 1962), the total luminosity is expected to increase little during helium burning, so that the structure of the envelope (and hence of the semiconvective zone) will change very slowly; the outward motion of q_s is also rather slow. Thus the star could probably accommodate quietly the sharp increase in X, despite the narrowness of the shell source. However, it seems unlikely that the inner edge of the semiconvective zone will ever penetrate the shell before the whole envelope becomes convective during the rightward swing of the evolutionary track in the H-R diagram toward red, carbon-burning models. We need only worry about possible hydrogen flaring in stars of mass greater than 30 $M_\odot$.

The evolution on the theoretical H-R diagram is shown in Figure 10 for the phases considered in this paper. The ages are given in units of 10^4 years. At $\tau = 9.07$ the spectral class becomes B0, and at $\tau = 9.67$ it is B3. The star is expected never to return to the region of O stars during its active life.

It is a pleasure to thank Dr. Robert Jastrow for the hospitality of the Institute for Space Studies. I gratefully acknowledge holding a Harvard scholarship during the academic year 1962–1963.

REFERENCES

Haselgrove, C. B., and Hoyle, F. 1956, *M.N.*, **116**, 515.
Hayashi, C., and Cameron, R. C. 1962, *Ap. J.*, **136**, 166.
Hayashi, C., Hoshi, R., and Sugimoto, D. 1962, *Prog. Theoret. Phys. Suppl* (Kyoto), No. 22.
Hayashi, C., Nishida, M., and Sugimoto, D. 1962, *Prog. Theoret. Phys.* (Kyoto), **27**, 1233.
Hofmeister, E., Kippenhahn, R., and Weigert, A. 1963, Stellar Evolution Conference (Goddard Institute for Space Studies, New York).
Hoyle, F. 1960, *M.N.*, **120**, 22.
Kushwaha, R. S. 1957, *Ap. J.*, **125**, 242.
Polak, E. J. 1962, *Ap. J.*, **136**, 465.
Reeves, H. 1962, *Stellar Energy Sources* (Goddard Institute for Space Studies, NASA Report).
Reiz, A. 1963, Stellar Evolution Conference (Goddard Institute for Space Studies, New York).
Sakashita, S., Ôno, Y., and Hayashi, C. 1959, *Prog. Theoret. Phys.* (Kyoto), **21**, 315.
Schwarzschild, M. 1958, *Structure and Evolution of the Stars* (Princeton, N.J.: Princeton University Press).
Schwarzschild, M., and Härm, R. 1958, *Ap. J.*, **128**, 348.
Schwarzschild, M., and Selberg, H. 1962, *Ap. J.*, **136**, 150.
Stothers, R. 1963, *Ap. J.*, **138**, 1074 ("Paper I").

© American Astronomical Society • Provided by the NASA Astrophysics Data System